On the effect of manufacturing imperfections and internal damage on the collapse strength of tubes: a nonlinear perspective

Lucas P. Gouveia, Eduardo N. Lages, Eduardo T. Lima Junior

Laboratory of Scientific Computing and Visualization, Center of Technology, Federal University of Alagoas
Av. Lourival Melo Mota, S/n, 57072-970, Alagoas, Brazil
lucasgouveia@lccv.ufal.br, enl@lccv.ufal.br, limajunior@lccv.ufal.br

Abstract. The estimation of critical external pressure of tubes is a nontrivial problem, particularly when considering the presence of damage, such as mechanical or chemical, and, manufacturing imperfections, such as cross-section ovality and eccentricity. This study presents the findings obtained from a nonlinear finite element analysis of 2-D tube cross-sections subjected to collapse pressures. The collapse strength of the tubes can vary significantly with modifications to the parameters related to the geometric disposition of the damage and imperfections. The study is carried out adopting configurations that are commonly observed in casing tubulars of oil and gas wells. Therefore, the results can support the design and integrity analysis of casing strings, improving knowledge about their behavior under well service conditions. The study is performed using Abaqus software with a Python scripting interface, enabling efficient evaluation of various geometric inputs. The nonlinear solver employs a load increment approach, causing the system to become unstable upon reaching the critical load. The load increments and displacements were carefully adjusted to maintain equilibrium using the arc length methodology (known as the Riks Method in the software). Different equilibrium trajectory shapes can arise depending on the initial geometric configuration, leading to diverse conclusions. For example, an increase in the separation angle between the ovality reference location and eccentricity reference location can decrease the collapse strength of thick tubes but increase it for thin tubes. Several other insights can be drawn from this study. Finally, a brief case study is presented, comparing the results with widely used equations in the well casing design practice.

Keywords: FEA, Klever Tamano model, buckling, casing design, casing wear.

1 Introduction

Numerical techniques play a crucial role in modeling physical phenomena, particularly when conducting laboratory tests is challenging due to high associated costs or when accessing a structural element in service is impractical. Many works in the literature have dedicated efforts to estimate the strength of damaged tubes, whether due to tool joint wear, uniform corrosion, or localized corrosion. However, the damages identified using ultrasonic inspection data in Gouveia et al. [1] exhibit a pattern that none of these studies have examined, comprising multiple damages. Additionally, simulations of wear prediction using the stiff-string model (Mitchell and Samuel [2]) have indicated that during subsequent drilling operations, there may be several contact points across the cross-section.

The residual collapse strength of damaged tubes depends on various parameters, such as the number of damages, their depth, extent, length, and position, as well as the properties of the intact tube, such as the cross-section slenderness ratio (OD/wt, outer diameter to wall thickness ratio), and the initial ovality and eccentricity. In literature, one can find works that perform experimental collapse tests (Kuriyama et al. [3], Sakakibara et al. [4], Liang and Li [5], Moreira Junior et al. [6]), usually relying on them to validate Finite Element Analysis (FEA). In addition to collapsing the tubes within a pressurized chamber, it is also necessary to machine the wear and accurately inspect the element. Variations in the applied methodologies and equipment can lead to non-comparable results among themselves.

FEA simulations are typically employed to generate an extrapolated dataset, enabling the investigation of the damaged tube behavior under various configurations. Sakakibara et al. [4], Wang et al. [7], and Lin et al. [8] conclude that 2-D modeling yields results very similar to 3-D modeling when the damage extends predominantly in the radial direction of the tube. The assumptions of single damage and constant damage width, made in these works, are reviewed in Mencaglia et al. [9] and Teigland et al. [10]. Differences of about 10% in the residual

strength estimative were observed for the same damage depth. Nevertheless, the proposed analytical equations based on the laboratory tests and FEA simulations carry all these uncertainties in their estimates.

This work presents results of nonlinear FEA modeling for two-dimensional cross sections of damaged tubes. It is investigated the effect of varying the initial geometric configuration concerning the positions of ovality, eccentricity and a groove-shaped damage in the inner wall of the tube. The insights gained from these results contribute to a better understanding of collapse studies involving damaged tubes.

2 FEA modeling

The collapse phenomenon in tubes ranging from thin to intermediate sizes presents instability issues marked by significant displacements and rotations. In such analyses, the approach involves solving the problem through small load increments, aimed at capturing the overall nonlinear behavior. Nevertheless, the deformed configuration that arises from each incremental load does not always align with the equilibrium path of the system. To manage this situation, iterations are undertaken, modifying the load and/or displacements to converge toward the equilibrium path (Leon et al. [11]). Among the various techniques, the Riks method, known as the arc-length method, is utilized, enabling concurrent control over both load and displacement. The simulation is configured with an initial unitary reference pressure, thus resulting in the load proportionality factor (LPF) being equal to the total collapse pressure.

The complete process is simulated using the Abaqus software (Smith [12]). The modeling incorporates boundary conditions and loads to replicate the conditions of a collapse test conducted within a hyperbaric chamber. As a result, the external load acting on the tube follows a hydrostatic distribution along its outer surface, while internal loading remains set equal to zero. A two-dimensional FEA modeling is employed, utilizing a ring-shaped configuration with plane strain conditions. To restrict movement, a distributed coupling mechanism is applied, linking the surface nodes to a reference point (RP) positioned at the geometric center of the cross-section. An 8-node hybrid biquadratic element, with reduced integration (CPE8RH), is adopted.

The true stress-strain relationship is described by an elastoplastic model with nonlinear hardening, as proposed by Silva [13] and based on ASME (American Society of Mechanical Engineers) guidelines. The failure criterion considers the maximum load capacity of the element. Upon reaching this point, the element becomes unstable, and the solution step provides negative load increments. The mesh convergence analysis involved multiple tube geometries, determining that 12 radial elements yield sufficiently accurate estimations in comparison to the 20 radial elements. The average runtime for each simulation is approximately 60 seconds.

For performing simulations with various configurations of damaged tube geometries, the Abaqus Python Scripting (Dassault Systemes Simulia Corporation [14]) is utilized to automate tasks such as model generation, processing, and post-processing. This architecture is designed for Python integration, enabling easy collaboration with other programming modules. Data input, information exchange, and output results are consistently managed through JavaScript Object Notation (JSON) files.

The model validation is performed comparing the outcomes with the equation proposed by Klever and Tamano [15] (referred to as KT). The API TR 5C3 (2018) [16] conducted a study indicating that this equation provided a better estimation of collapse strength of tubes compared to other equations in the literature. The comparative dataset contains 2,986 collapse test results, comprising several tube geometries and metallurgies from various manufacturers globally. The metric used to evaluate the quality of equations is the model uncertainty, representing the ratio between the actual (test) strength and the strength predicted by the equation. The average model uncertainty for KT is 0.9991, with a standard deviation of 6.70%, being well suited as a gaussian distribution.

Figure 1 illustrates the collapse strength estimations from both the numerical model (points) and the KT equation (curves incorporating means and 5%, 25%, 75%, and 95% percentiles). It is evident a convergence across most of the results for the three steel grades in the study: K-55, N-80 and P-110. However, for a cross-sectional slenderness ratio of 10 (thick-walled tubes) across all three steel grades, the FEA simulation produces higher strengths than the P95 of KT. This can be attributed to the allowance of FEA modeling for plastic deformation of the material. The remaining divergences observed may rely on several factors linked to simplifications adopted in the simulation, including 2-D modeling, idealized ellipse geometry for inner and outer walls, relative position between ovality and eccentricity, among others. Additionally, the KT results themselves contain inherent uncertainties originating from tests conducted by different manufacturers. In conclusion, FEA modelling provides

appropriate results for the proposed study.

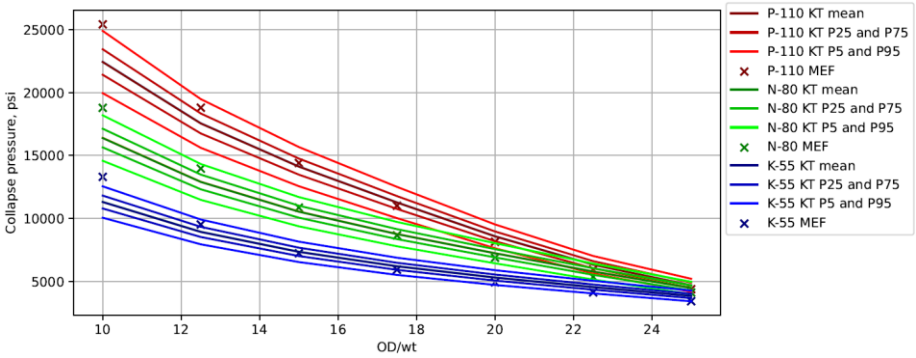

Figure 1. Results of FEA modelling and the KT equation for intact tubes with average parameters from API TR 5C3 (2018).

3 Results and discussion

The results are presented in two main topics: effect of initial configuration of intact tubes and effects of initial configuration of damaged tubes. All cases are carried out considering API TR 5C3 (2018) mean values for ovality ($ov = 0.217\%$) and eccentricity ($ecc = 3.924\%$).

3.1 Intact tubes

Collapse modeling for intact tubes is performed to verify the behavior with different OD/wt and with variations in the ovality and eccentricity relative positions. In the first study, values of OD/wt of 10, 17.5, and 25 are adopted with P-110 steel grade. The second analysis expands the conclusions to K-55 and N-80 grades. Figure 2 presents the simulation results at failure, along with the LPF behavior over the arc length increments. It is noticeable that, at failure point, only the thickest tube reaches stresses exceeding the material's yield limit (110,000 psi). The other two tubes become unstable before that, indicating loss of integrity in the elastic regime. Different shapes of arc length vs. LPF curves arise, demonstrating that distinct equilibrium paths occur over the load increments. There seems to be a more pronounced smoothing of the transition from the linear region to the load damping region in the curves for slender tubes.

Next, the influence of the position of the maximum external radius $\theta_{r\,max}$ in relation to the maximum thickness $\theta_{wt\,max}$ of the cross-section is analyzed. These two parameters define the location of manufacturing imperfections in the tube, ovality and eccentricity. For ease of visualization, examples of sections with ovality and eccentricity defined at different positions are presented in Fig. 3. The intensities are magnified for clarity.

In the left plot of Fig. 4, it is presented the ratio of the collapse-resistant pressure in relation to the reference case $\theta_{r\,max} - \theta_{wt\,max} = 0$. It is observed that due to the symmetries of ovalized and eccentric tubes, the strength behavior also tends to exhibit symmetry. Additionally, it is noted that the reference configuration is not always the one resulting in the lowest strength. Some tubes achieve minimum strength when $\theta_{r\,max}$ and $\theta_{wt\,max}$ are positioned perpendicular to each other. In the right plot of Fig. 4, the maximum von Mises stress recorded at the point of failure is depicted. Only the three tubes with an OD/wt ratio of 10.0 exceed the steel yield limit. The other cases fail before reaching the yield stress. According to Clinedinst [17], when this occurs, instability-induced failure is characterized, also known as cross-sectional buckling failure. Tubes that fall under this category appear to exhibit varied behavior in terms of ovality and eccentricity positioning, potentially showing strength gain or loss. This can be attributed to the different equilibrium paths that can be taken when the system becomes unstable. On the other hand, tubes that fail above the yield limit consistently show strength loss, with the minimum at 90º or 270º.

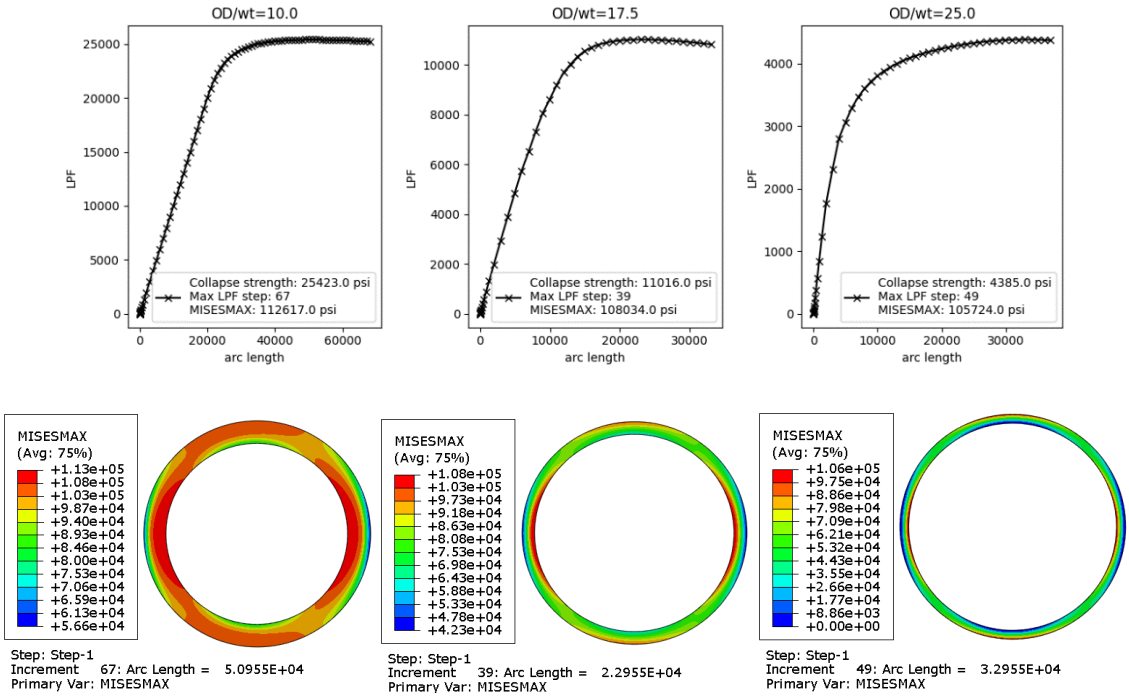

Figure 2. Equivalent stress distribution for intact tubes at the collapse failure moment and the LPF curve as a function of arc length increments.

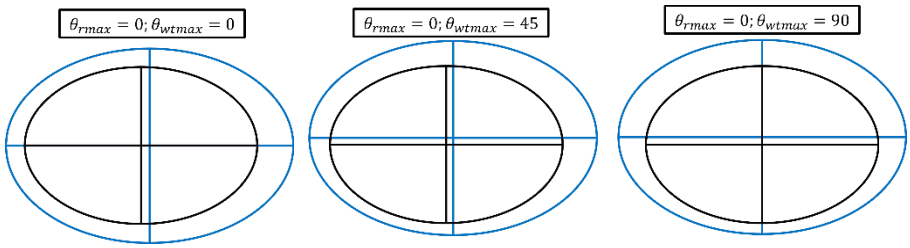

Figure 3. Cross-sectional magnified geometries with ovality and eccentricity positioned in different ways, but with the same magnitudes.

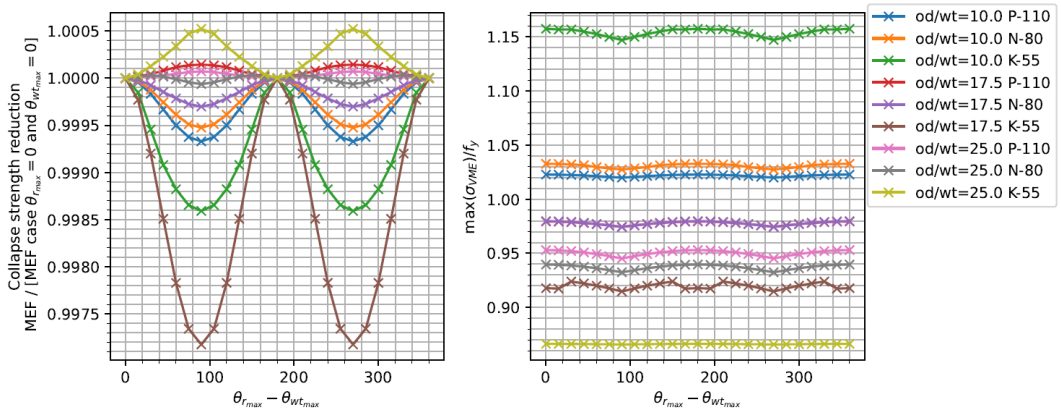

Figure 4. Study of the influence of the positioning of maximum radius and maximum thickness in the cross-section.

Figure 5 depicts the cases of grade K-55 with OD/wt ratios of 17.5 and 25, where strength loss and gain were observed depending on ovality and eccentricity configuration. Configurations with zero separation and

perpendicular separation are used to generate the LPF curves vs. arc length. It is noticeable that the curves distinctly differ in shape for different OD/wt ratio, indicating that different instability modes lead to tube collapse. Thus, for each mode, the behavior differs as the separation between maximum radius and maximum thickness changes.

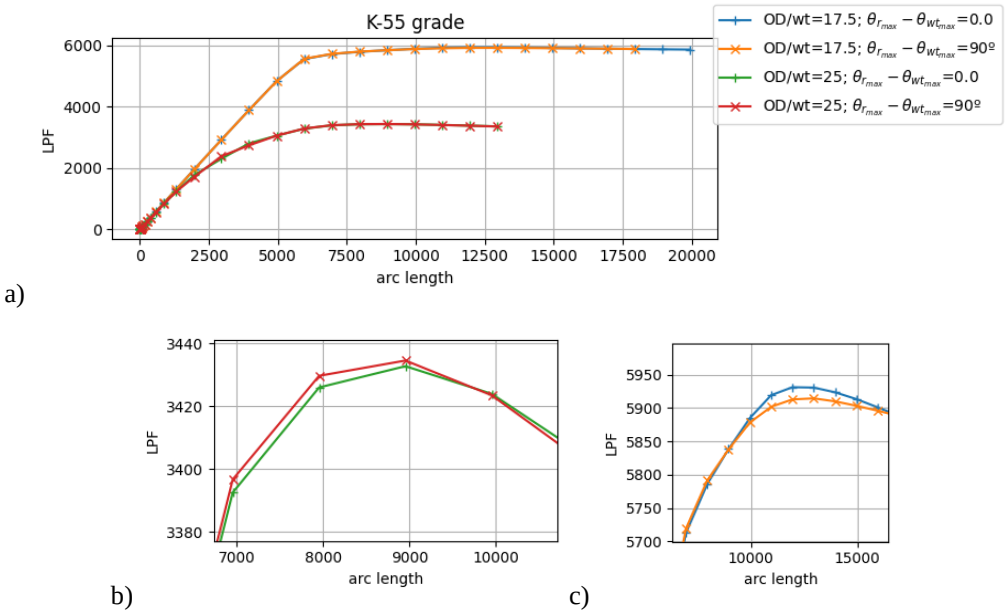

Figure 5. Behavior of the LPF curves vs. arc length in specific cases of grade K-55 in the study of variation in ovality and eccentricity positioning: a) overall view; b) detail of the maximum points of the curves for OD/wt=25; c) detail of the maximum points of the curves for OD/wt=17.5.

It is important to highlight that, in general, the error in adopting the perpendicular separation is small, not exceeding 20 psi (-0.3%) in favor of safety and 2 psi (0.05%) against safety, in the most critical cases. Thus, the 0º separation is maintained in the following cases, aiming to simplify the analyses.

3.2 Effect of grooved-shape damage location

Further analysis considers the effect of varying the position of a grooved-shape damage in the cross-section. No study was found in the literature that addresses this issue by relating this position with the positions of maximum external radius and thickness. The groove depth remains fixed at 10% of the nominal wall thickness, and the width of the damage corresponds to a circle with a radius equal to 50% of the internal radius. Figure 6 presents the results with strength reduction on the left and maximum von Mises stress on the right. A symmetry of the responses around 180º is evident, as expected. Tubes show a strength gain up to 90º, and intriguingly, some of them even surpass the strength of the intact tube. Only tubes with an OD/wt ratio of 10 do not surpass the reference value.

To understand the strength gain with the introduction of damage, Fig. 7-a) compares the results of a P-110 tube with OD/wt ratio of 17.5, both without and with damage, at 90° and 180°. It is noticeable that in the case of $\theta_{damage} = 90°$, the shape of the LPF curve undergoes a sharper transition to the maximum plateau. This leads to a different equilibrium path and, consequently, a change in the instability mode, resulting in a higher critical load case compared to the tube without damage. This example emphasizes the complexity of modeling the collapse of damaged tubes, where different initial configurations can lead to non-trivial responses. Comparing the configurations at the point of failure for the tube without damage (Fig. 7-b)) and with damage at 90° (Fig. 7-c)), it can be observed that the damage seems to somewhat relieve stress on the external wall at 90°, balancing it with the inner wall. In the opposite direction, in the case of $\theta_{damage} = 180°$ (Fig. 7-d)), the damage seems to contribute even more to stresses rising rapidly at 180°. This causes the element to reach the unstable point earlier, reducing residual resistance.

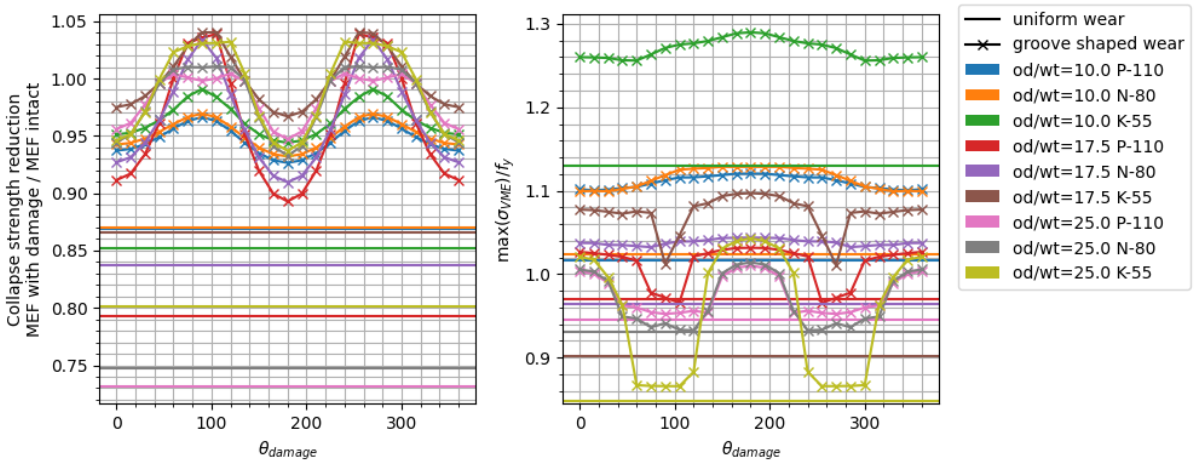

Figure 6. Effect of the position of a damage consuming 10% of the wall thickness in nine tubes.

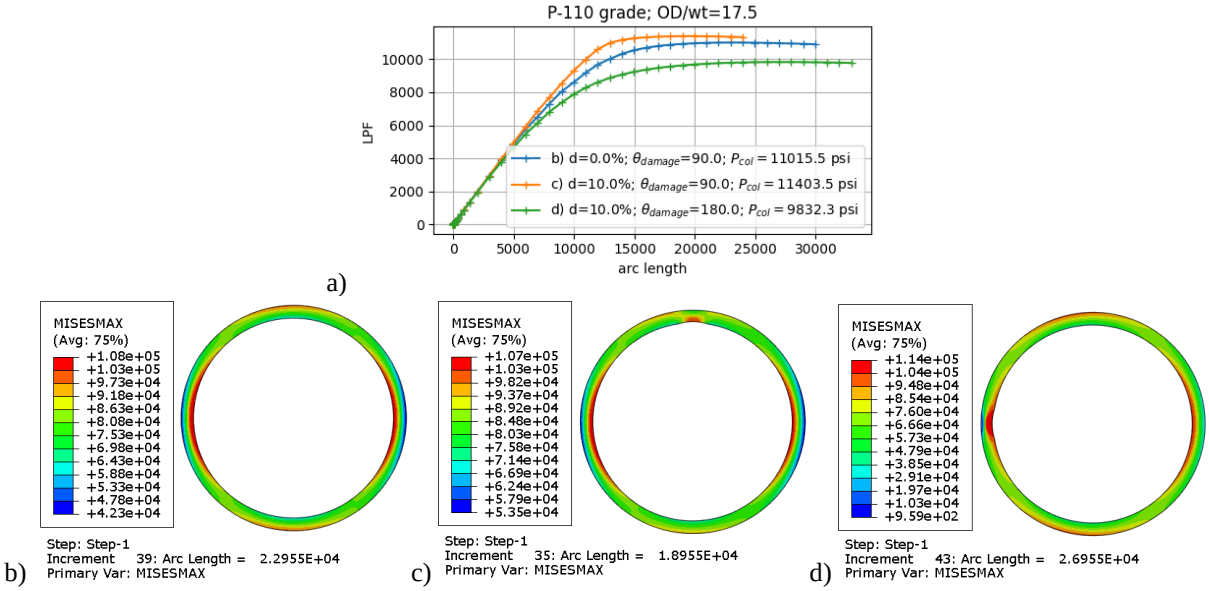

Figure 7. Comparison of damaged tube cases with variable damage locations.

Hence, it is interesting to highlight that certain cases exhibit a considerable strength variation solely due to the position of the groove. In the most critical scenarios, this maximum variation can be close to 15%, which means that altering the damage position by 90° could result in a difference of up to 1888 psi in residual tube strength. Furthermore, it is worth noting that no model in the literature considers the influence of this position in the cross-section. This magnitude is likely to be smaller when the ovality and eccentricity intensities of the cross-section are lower than API values, which is expected given the manufacturing processes of modern pipes.

4 Conclusions

This work presented results of nonlinear FEA modeling for two-dimensional cross sections of intact and damaged tubes. It was investigated the effect of varying the initial geometric configuration concerning the positions of ovality, eccentricity and a groove-shaped damage in the inner wall of the tube. It can be highlighted that ovality and eccentricity relative positions do not significantly alter the collapse strength estimate of intact tubes. On the other hand, some damage locations provide residual strengths estimates with a considerable difference of others even when the damage intensity is the same.

Acknowledgements. The authors acknowledge the financial and technical support provided by Petróleo Brasileiro S.A. - PETROBRAS. The second author would also like to thank CNPq for the financial support.

Authorship statement. The authors hereby confirm that they are the sole liable persons responsible for the authorship of this work, and that all material that has been herein included as part of the present paper is either the property (and authorship) of the authors or has the permission of the owners to be included here.

References

[1] Gouveia, L. P. et al. "Casing wear log using a prewear ellipse shape from ultrasonic logging data". SPE Journal, v. 27, n. 5, pp. 2642–2654.
[2] Mitchell, R. F.; Samuel, R. How good is the torque-drag model? In: Proceedings - *SPE/IADC Drilling Conference 24*, p. 232–240, 2009.
[3] Kuriyama, Y. et al. Effect of wear and bending on casing collapse strength. In: Proceedings - *SPE Annual Technical Conference and Exhibition*, 1992.
[4] Sakakibara, N.; Kyriakides, S.; Corona, E. Collapse of partially corroded or worn pipe under external pressure. *International Journal of Mechanical Sciences*, v. 50, n. 12, pp. 1586–1597, 2008.
[5] Liang, E. G.; Li, Z. F. Computation model for collapse strength of the casing wear. *Advanced Materials Research*, v. 403-408, pp. 496–501, nov 2011.
[6] Moreira Junior, N. M. et al. Worn pipes collapse strength: experimental and numerical study. *Journal of Petroleum Science and Engineering*, Elsevier, v. 133, pp. 328–334, 2015.
[7] Wang, T. et al. Investigation of the ultimate residual strengthen of a worn casing by using the arc-length algorithm. *Engineering Failure Analysis*, v. 28, p. 1–15, mar 2013.
[8] Lin, B. et al. Accurate prediction of casing collapse resistance by 3d finite element modeling. *IADC/SPE International Drilling Conference and Exhibition*, Galveston, Texas, USA, March 2022.
[9] Mencaglia, X. et al. Towards a novel approach to consider casing wear in well designs. *Offshore Technology Conference*, Houston, Texas, USA, May 2022.
[10] Teigland, A. et al. A generalized empirical expression for the collapse of worn tubulars with a crescent-shaped wear groove under combined loads. *Journal of Petroleum Science and Engineering*, v. 208, p. 109187, 2022.
[11] Leon, S. E. et al. A Unified library of nonlinear solution schemes. *Applied Mechanics Reviews*, v. 64, n. 4, jul 2011.
[12] Smith, M. ABAQUS/Standard User's Manual, Version 6.9. 2009.
[13] Silva, G. T. da. Análise numérica da resistência ao colapso em tubulares de revestimento de poços dotados de imperfeições de manufatura e desgaste. 123 p. Thesis — Federal University of Alagoas, 2020.
[14] Dassault Systemes Simulia Corporation, 2011, "Abaqus 6.11 Scripting User's Manual", Dassault Systemes Simulia Corporation.
[15] Klever, F., & Tamano, T., 2006, "A new octg strength equation for collapse under combined loads", *SPE Drilling & Completion*, v. 21, n. 03, pp. 164–179.
[16] American Petroleum Institute. API/TR 5C3: Calculating performance properties of pipe used as casing or tubing, 2018.
[17] Clinedinst, W. O. Collapse resistance of pipe. Thesis (PhD) — Century University, 1985.